

# MG53 Regulates Membrane Budding and Exocytosis in Muscle Cells<sup>\*S</sup>

Received for publication, November 21, 2008 Published, JBC Papers in Press, November 24, 2008, DOI 10.1074/jbc.M808862000

Chuanxi Cai<sup>†1,2</sup>, Haruko Masumiya<sup>§1</sup>, Noah Weisleder<sup>†1</sup>, Zui Pan<sup>‡</sup>, Miyuki Nishi<sup>§¶</sup>, Shinji Komazaki<sup>||</sup>, Hiroshi Takeshima<sup>§¶3</sup>, and Jianjie Ma<sup>†\*\*\*4</sup>

From the Departments of <sup>†</sup>Physiology and Biophysics and <sup>\*\*</sup>Medicine, Robert Wood Johnson Medical School, Piscataway, New Jersey 08854, <sup>§</sup>Department of Medical Chemistry, Tohoku University Graduate School of Medicine, Miyagi 980-8575, Japan, <sup>¶</sup>Department of Biological Chemistry, Kyoto University Graduate School of Pharmaceutical Sciences, Kyoto 606-8501, Japan, and <sup>||</sup>Department of Anatomy, Saitama Medical University, Saitama 350-0495, Japan

Membrane recycling and remodeling contribute to multiple cellular functions, including cell fusion events during myogenesis. We have identified a tripartite motif (TRIM72) family member protein named MG53 and defined its role in mediating the dynamic process of membrane fusion and exocytosis in striated muscle. MG53 is a muscle-specific protein that contains a TRIM motif at the amino terminus and a SPRY motif at the carboxyl terminus. Live cell imaging of green fluorescent protein-MG53 fusion construct in cultured myoblasts showed that although MG53 contains no transmembrane segment it is tightly associated with intracellular vesicles and sarcolemmal membrane. RNA interference-mediated knockdown of MG53 expression impeded myoblast differentiation, whereas overexpression of MG53 enhanced vesicle trafficking to and budding from sarcolemmal membrane. Co-expression studies indicated that MG53 activity is regulated by a functional interaction with caveolin-3. Our data reveal a new function for TRIM family proteins in regulating membrane trafficking and fusion in striated muscles.

When myoblasts exit the cell cycle during myogenesis, dramatic changes in membrane organization occur as myoblast fusion allows the formation of multinucleated muscle fibers. In addition to cell fusion events, differentiation of myotubes involves establishment of specialized membrane structures (1, 2). The transverse tubular invagination of sarcolemmal membrane and the intracellular membrane network known as the sarcoplasmic reticulum are two highly organized membrane architectures in cardiac and skeletal muscle. Establishment of these intricate membrane compartments requires extensive

remodeling of the immature myoblast membranes. Dynamic membrane remodeling also contributes to many physiologic processes in mature muscle, including  $\text{Ca}^{2+}$  signaling, trafficking of glucose transporter (GLUT4), and other membrane internalization events involving caveolae structures (3–6). Although defects in membrane integrity have been linked to various forms of muscular dystrophy (7, 8), the molecular machinery regulating these specific membrane recycling and remodeling events in striated muscle is not well defined.

The large tripartite motif (TRIM)<sup>5</sup> family of proteins is involved in numerous cellular functions in a wide variety of cell types. Members of this protein family contain signature motifs that include a RING finger, a zinc binding moiety (B-box), and a coiled coil structure (RBCC), which invariably comprise the amino-terminal domain of TRIM family members (9). The carboxyl-terminal sequence of TRIM proteins is variable; in some cases a subfamily of TRIM proteins contains a SPRY domain, a sequence first observed in the ryanodine receptor  $\text{Ca}^{2+}$  channel in the sarcoplasmic reticulum membrane of excitable cells (10). Extensive studies have revealed that protein-protein interactions in the cytosol mediate the defined functions of TRIM proteins. For example, the ubiquitin E3 ligase enzymatic activity of several TRIM family members requires the B-box motif (11, 12). Recent studies have also indicated a role for TRIM proteins in defense against events involving membrane penetration, such as protection against infection by various viruses, including human immunodeficiency virus (13–15). Although most of the studies concentrate on the cytosolic action of TRIM, limited reports have investigated the role of TRIM proteins in membrane signaling or recycling.

We have previously established an immunoproteomics approach that allows definition of novel components involved in myogenesis,  $\text{Ca}^{2+}$  signaling, and maintenance of membrane integrity in striated muscle (16). Using this approach, we have shown that junctophilin is a structural protein that establishes functional communication between sarcoplasmic reticulum and transverse tubule membranes at triad and dyad junctions in striated muscle (17–19). Further studies identified mitsugumin 29, a synaptophysin-related protein that is essential for biogen-

<sup>\*</sup> This work was supported, in whole or in part, by National Institutes of Health grants (to J. M. and N. W.). This work was also supported by grants from the Chinese Natural Science Foundation (to J. M.) and the Ministry of Education, Science, Sports and Culture of Japan (to H. T.). The costs of publication of this article were defrayed in part by the payment of page charges. This article must therefore be hereby marked “advertisement” in accordance with 18 U.S.C. Section 1734 solely to indicate this fact.

<sup>S</sup> The on-line version of this article (available at <http://www.jbc.org>) contains supplemental Movies 1 and 2 and Tables 1 and 2.

<sup>1</sup> These authors contributed equally to this work.

<sup>2</sup> Recipient of a postdoctoral fellowship from the American Heart Association.

<sup>3</sup> To whom correspondence may be addressed. Tel.: 81-75-753-4572; Fax: 81-75-753-4605; E-mail: [takeshim@pharm.kyoto-u.ac.jp](mailto:takeshim@pharm.kyoto-u.ac.jp).

<sup>4</sup> To whom correspondence may be addressed: Dept. of Physiology and Biophysics, Robert Wood Johnson Medical School, 675 Hoes Lane, Piscataway, NJ 08854. Tel.: 732-235-4494; Fax: 732-235-4483; E-mail: [maj2@umdnj.edu](mailto:maj2@umdnj.edu).

<sup>5</sup> The abbreviations used are: TRIM, tripartite motif; GFP, green fluorescent protein; RBCC, a RING finger, a zinc binding moiety (B-box), and a coiled coil structure; E3, ubiquitin-protein isopeptide ligase; CHO, Chinese hamster ovary; shRNA, small hairpin RNA; M-BCD, methyl- $\beta$ -cyclodextrin; cav, caveolin; SPRY, SPla and ryanodine receptor.

esis of triad membrane structures and  $\text{Ca}^{2+}$  signaling in skeletal muscle (20, 21). Screening of this immunoproteomics library led to the recent identification of MG53, a muscle-specific TRIM family protein (22). Domain homology analysis revealed that MG53 contains the prototypical RBCC motifs plus a SPRY domain at the carboxyl terminus. Genetic knock-out and functional studies reveal that MG53 nucleates the assembly of the sarcolemmal membrane repair machinery to restore cellular integrity following acute damage to the muscle fiber (22).

Here we present evidence illustrating that MG53, in contrast to other known TRIM proteins, can localize to intracellular vesicles and the sarcolemmal membrane. A functional interaction between MG53 and caveolin-3, another muscle-specific protein, plays an essential role in regulating the dynamic process of membrane budding and exocytosis in skeletal muscle.

## EXPERIMENTAL PROCEDURES

**Plasmid Construction**—The full-length mouse MG53 cDNA and associated truncation mutants were generated by PCR using the primers described in supplemental Table 1. For construction of pCMS-MG53, after digestion by the appropriate restriction enzymes, the PCR-amplified cDNA was inserted into pCMS-EGFP vector (Invitrogen) at NheI/XbaI sites. For construction of GFP-MG53, GFP-TRIM, GFP-SPRY, MG53-GFP, TRIM-GFP, and SPRY-GFP, PCR products were inserted into pEGFP-C1 at the XhoI/XbaI sites or pEGFP-N1 at the XhoI/KpnI sites.

**Cell Culture**—The C2C12 myoblast cell line was purchased from the American Type Culture Collection (Manassas, VA). Cells were grown in a humidified environment at 37 °C and 5%  $\text{CO}_2$  in Dulbecco's modified Eagle's medium for C2C12 or Ham's F-12 medium for Chinese hamster ovary (CHO) cells supplemented with 10% fetal bovine serum, 100 units/ml penicillin, and 100  $\mu\text{g}/\text{ml}$  streptomycin. To induce myotube differentiation, C2C12 myoblasts were grown to confluence, and the medium was switched to Dulbecco's modified Eagle's medium containing 2% horse serum, 100 units/ml penicillin, and 100  $\mu\text{g}/\text{ml}$  streptomycin. For transient transfections, C2C12 myoblasts or CHO cells were plated at 70% confluence in glass-bottomed dishes. After 24 h, cells were transfected with plasmids described above using GeneJammer reagent (Stratagene). Cells were visualized by live cell confocal imaging at 24–48 h after transfection or at times indicated for individual experiments. In some experiments, C2C12 myoblasts were allowed to differentiate into myotubes for the indicated time before observation.

**Immunostaining and Electron Microscopy**—Immunocytochemical analyses using mAb5259 were carried out as described previously (23). For MG53 expression in amphibian embryonic cells, cRNA for rabbit MG53 was prepared using a commercial kit (Megascript, Ambion). Newt embryos (1–8 cell stages) were injected with cRNA (~70 ng/embryo), incubated for a day, and analyzed using electron microscopy as described previously (24). For tracking the endocytosis using cationic ferritin, a solution containing 10 mg/ml cationic ferritin (cationic ferritin-N,N-dimethyl-1,3-propanediamine, Sigma) and 0.15 M NaCl was injected into the blastocoelic cavity of embryos (~0.6  $\mu\text{l}/\text{embryo}$ ).

**Live Cell Imaging**—To monitor intracellular trafficking of GFP-MG53, CHO or C2C12 cells were cultured in glass-bottomed dishes (Biopetechs Inc.) and transfected with the plasmids described above. Fluorescence images were captured at 3.18 s/frame using a Bio-Rad 2100 Radiance laser scanning confocal microscope with a 63 $\times$  1.3 numerical aperture oil immersion objective.

**RNA Interference Assay**—The target sequence for small hairpin RNA (shRNA) knockdown of MG53 is at position 622–642 (GAG CTG TCA AGC CTG AAC TCT) in the mouse MG53 cDNA. For caveolin-3, the target sequence is at position 363–380 (GAC ATT CAC TGC AAG GAG ATA). Complementary sense and antisense oligonucleotides were synthesized using sequences described in supplemental Table 2. To construct the MG53 shRNA and control plasmids, annealed oligonucleotides were inserted into psiRNA-hH1GFPzeo G2 (InvivoGene) at the Acc65I/HindIII restriction enzyme sites. For caveolin-3 shRNA and control plasmids, annealed oligonucleotides were inserted into pRNAiDsRed vector (BD Biosciences) at the EcoRI/BamHI restriction enzyme sites. Each vector has a fluorescent protein expression cassette (green or red) under control of a separate promoter that acts as a marker of cell transfection. All plasmids were confirmed by direct sequencing with flanking primers, and the down-regulation of MG53 and caveolin-3 protein expression was examined by Western blot analysis.

**Western Blot and Co-immunoprecipitation**—C2C12 or CHO cells were harvested and lysed with ice-cold modified RIPA buffer (150 mM NaCl, 5 mM EDTA, 1% Nonidet P-40, 20 mM Tris-HCl, pH 7.5) in the presence of a mixture of protease inhibitors (Sigma). 20  $\mu\text{g}$  of total protein were separated on a 4–12% SDS-polyacrylamide gel. Immunoblot of MG53 was performed with either mAb5259 or polyclonal anti-MG53 antibodies. A standard protocol was used for co-immunoprecipitation studies of MG53 and caveolin-3. In brief, skeletal muscle tissue or C2C12 myotubes were lysed in 0.5 ml of modified RIPA buffer. The whole cell lysate (500  $\mu\text{g}$ ) was incubated overnight with 5  $\mu\text{g}$  of polyclonal rabbit anti-MG53 or monoclonal anti-caveolin-3 antibody. As a negative control, 500  $\mu\text{g}$  of whole cell lysate was incubated with 5  $\mu\text{g}$  of normal rabbit or mouse IgG and processed as described above. The immune complexes were collected on protein G-Sepharose beads by incubating for 2 h and washed four times with RIPA buffer.

## RESULTS

**Overexpression of MG53 Produces Filopodia-like Structures in Both Excitable and Non-excitable Cells**—To elucidate the cell biological function of MG53, we expressed the MG53 cDNA in C2C12 myogenic cells as well as CHO cells. C2C12 cells at the myoblast stage do not express endogenous MG53 protein; however, differentiated C2C12 myotubes do express MG53. CHO cells are non-excitable epithelial cells that contain no endogenous MG53 protein. As shown in Fig. 1A, transient transfection of MG53 cDNA into C2C12 myoblasts or CHO cells produced the expression of a recombinant protein of 53 kDa that could be recognized by mAb5259. The molecular size of the recombinant protein is identical to the endogenous MG53 present in both rabbit and mouse muscles, thus confirming the identity of the isolated cDNA clone as MG53.



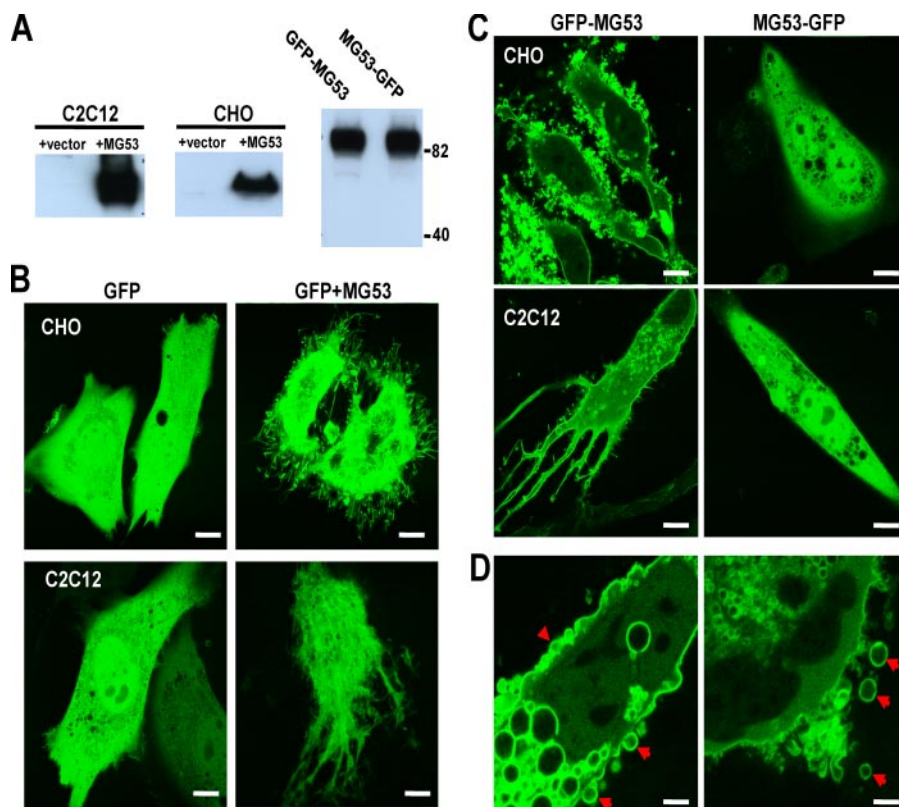


**FIGURE 1. Induction of filopodia-like structures with overexpression of MG53 in both muscle and non-muscle cells.** A, Western blot analysis shows the overexpression level of MG53 in C2C12 myoblasts (left panel) and CHO (middle panel) cells and also GFP-MG53 and MG53-GFP (right panel) in C2C12 myoblasts (20  $\mu$ g of total protein/lane). B, typical confocal images of CHO (upper panel) and C2C12 myoblasts (lower panel) transfected with GFP (left panel) or GFP + MG53 (right panel) revealing filopodia-like structures after overexpression of MG53. Scale bar, 5  $\mu$ m. C, confocal images of GFP-MG53 (left panel) and MG53-GFP (right panel) expressed in CHO cells (upper panel) and C2C12 myoblast (lower panel) revealing membrane targeting and intracellular vesicular distribution of MG53 as well as the appearance of filopodia-like structures. Scale bar, 5  $\mu$ m. D, magnified confocal images illustrating the intracellular vesicles, budding vesicles (left panel) on the plasma membrane, and extracellular vesicles near the vicinity (right panel). Scale bar, 1  $\mu$ m.

Co-transfection of cells with two plasmids containing cDNAs that encode either enhanced GFP or MG53 at a ratio of 10:1 provided a convenient method to identify transfected cells by fluorescence microscopy. With confocal microscopic imaging, we observed dramatic changes in morphology of cells transiently transfected with MG53 (Fig. 1B). Specifically extensions of the cell surface membranes formed distinct filopodia-like structures in both CHO cells and C2C12 myoblasts that transiently overexpress MG53.

To further examine the MG53-induced changes in cell morphology, we generated two GFP fusion constructs of MG53, GFP-MG53 and MG53-GFP, with attachment of GFP to the amino terminus or carboxyl terminus of MG53, respectively. Although both fusion proteins can be expressed in CHO cells and C2C12 myoblasts (Fig. 1A), the subcellular distribution and functional effects of GFP-MG53 and MG53-GFP were drastically different. Using confocal microscopy, we found that GFP-MG53 fusion proteins were localized to both intracellular vesicles and cell surface membranes in both CHO and C2C12 cells (Fig. 1C, left panels). This result is consistent with our electron microscopic localization of MG53 in skeletal muscle fibers (22) and suggests that MG53 may participate in membrane trafficking events in muscle cells.

Interestingly the distribution pattern of MG53-GFP fusion protein was mostly cytosolic in both CHO and C2C12 cells (Fig. 1C, right panels), which is in sharp contrast to the membrane-attached distribution of GFP-MG53. In addition, the extensive filopodia-like membrane extensions induced by overexpression of MG53 or GFP-MG53 was completely absent in cells transfected with MG53-GFP. Because shielding the carboxyl terminus of MG53 by fusion with GFP alters the subcellular distribution of MG53, it is likely that the SPRY motif at the carboxyl-terminal end of MG53 plays a role in anchoring MG53 to the different membrane compartments (see Fig. 7).

Live cell fluorescence imaging identified dynamic trafficking of intracellular vesicles and active exocytotic fusion and vesicle budding at the cell surface membrane in cells overexpressing GFP-MG53 (22). Close examination revealed the occurrence of vesicle fusion events at the surface membrane (Fig. 1D, left panel). Budding of vesicles containing GFP-MG53 could be clearly identified as well as released extracellular vesicles observed in the vicinity of transfected cells (Fig. 1D, right panel). Typically C2C12 myoblast cells could sustain GFP-MG53 overexpression for 48–72 h and exhibited a consistent pattern of GFP-MG53 vesicle trafficking. Prolonged overexpression of MG53 leads to progressive apoptosis due to disrupted intracellular  $\text{Ca}^{2+}$  homeostasis (not shown).

Although there is no membrane-spanning segment or lipid modification motif in its primary structure, MG53 appears to be primarily restricted to membrane structures in skeletal muscle based on several observations. First, MG53 was recovered in microsomal membrane vesicles but not in cytosolic fractions during biochemical fractionations of skeletal muscle tissues (not shown). Second, immunohistochemical analysis with mAb5259 showed specific labeling for MG53 in the sarcolemmal and transverse tubule membranes in longitudinal sections of skeletal muscle fibers (Fig. 2A). Moreover transverse sections revealed a localized concentration of MG53 near sarcolemmal membrane with a broader staining pattern than is typically observed for integral membrane proteins of the sarcolemma (Fig. 2B). A role for MG53 in intracellular membrane formation was confirmed in amphibian embryonic cells where injection of MG53 cRNA generated distinct intracellular vesicular structures that can be continuous with the extracellular space. Vesicle formation could be observed by electron microscopy in

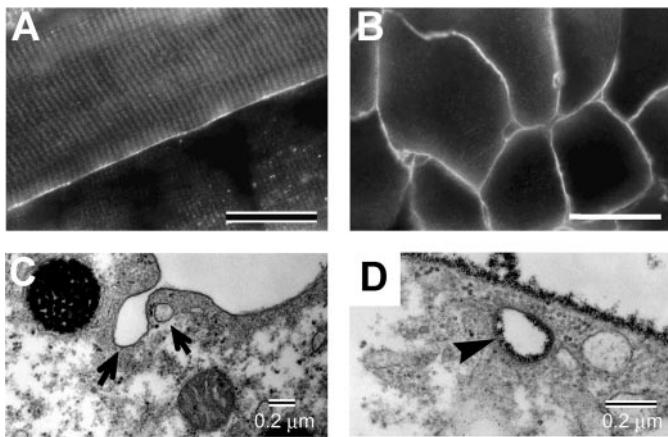


**FIGURE 2. MG53 localizes to sarcolemmal membrane and can produce vacuole formation.** *A*, representative immunofluorescence staining of longitudinal sections from rabbit skeletal muscle reveals tethering of MG53 near the transverse tubules and sarcolemmal membranes. Scale bar, 10  $\mu$ m. *B*, representative immunofluorescence staining of transverse sections from rabbit skeletal muscle reveals tethering of MG53 near sarcolemmal membranes. Scale bar, 10  $\mu$ m. *C*, amphibian embryos were injected with rabbit MG53 cRNA. Vesicle formation could be observed by electron microscopy in many cells expressing MG53. *D*, these vesicles could make contact with the extracellular space as illustrated by their ability to take up ferritin from the extracellular space (arrow).

many cells expressing MG53 (Fig. 2C). On average, vacuoles near the plasma membrane were frequently found in cells expressing MG53 ( $42.6 \pm 2.3\%$ , data from 21 embryos), which is significantly higher than those of control cells ( $4.7 \pm 1.5\%$  from 11 embryos,  $p < 0.001$ ). These vesicles could make contact with the extracellular space as illustrated by their ability to take up ferritin from the extracellular space (Fig. 2D, arrow).

**MG53 Contributes to Skeletal Muscle Myogenesis by Regulating Myoblast Differentiation**—To directly examine the role of MG53-mediated membrane fusion on the myogenesis of skeletal muscle, we used a specific RNA interference probe to knock down the expression of endogenous MG53 in differentiated C2C12 myotubes. The efficacy of an shRNA probe recognizing the nucleotide sequence 632–652 of the mouse MG53 cDNA in suppressing the expression of MG53 was assayed in CHO cells. For this study, CHO cells were transiently transfected with a 10:1 ratio of plasmids carrying either the shRNA-MG53 cDNA or the MG53 cDNA. As shown in Fig. 3A, a greater than 80% reduction of MG53 expression was observed in cells transfected with shRNA-MG53 as compared with cells transfected with a nonspecific shRNA probe.

Acute suppression of MG53 resulted in a marked decrease in C2C12 myotube differentiation (Fig. 3B). As a control, C2C12 myoblasts transfected with a nonspecific shRNA probe exhibited a normal differentiation pattern with numerous multinucleated myotubes present by day 5 following serum withdrawal. Mature myotubes were widely distributed by day 10 of differentiation. In contrast, C2C12 myoblasts transfected with the shRNA-MG53 probe formed significantly fewer myotubes at both day 5 and day 10 after serum deprivation-induced differentiation (Fig. 3C). These results suggest that normal expression of MG53 is necessary for the differentiation of C2C12 myoblasts into myotubes.

**Functional Interaction between MG53 and Caveolin-3 Regulates Dynamic Membrane Budding Process in Skeletal**

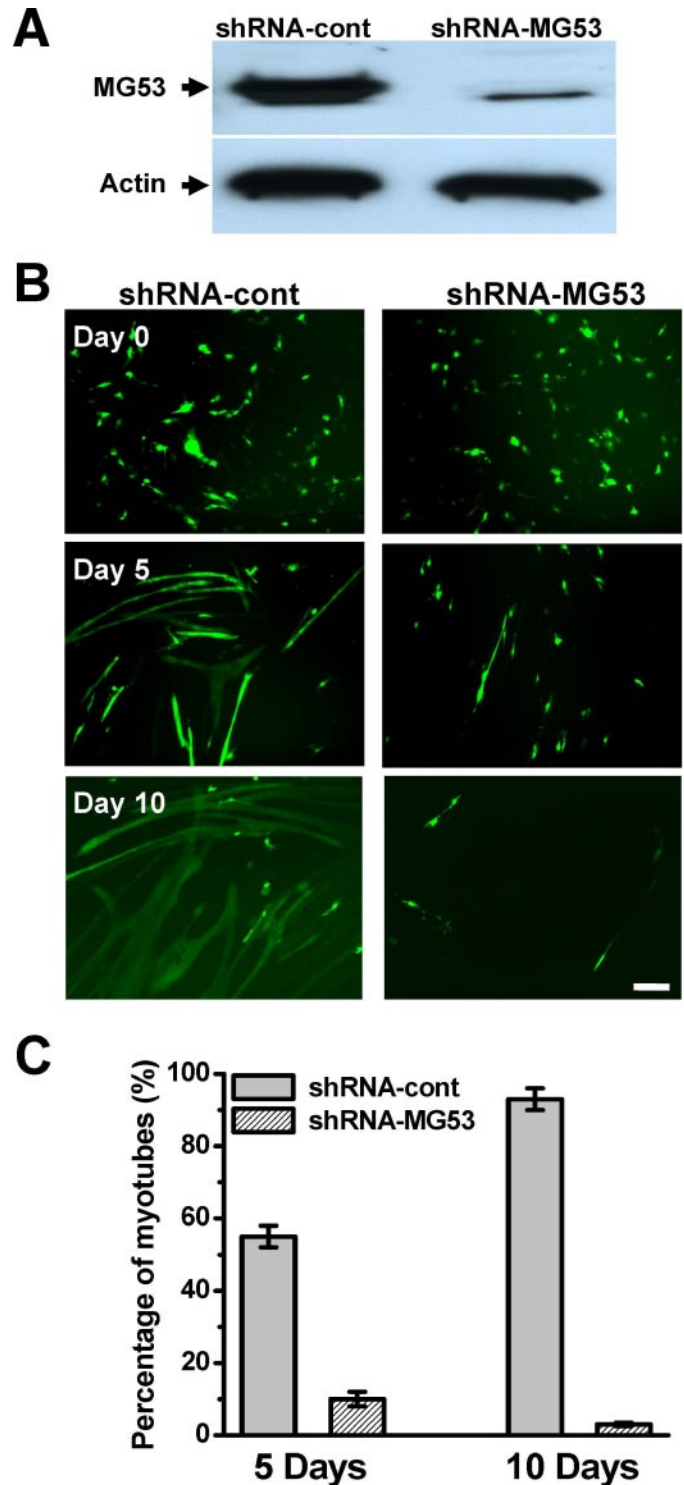


**FIGURE 3. MG53 contributes to skeletal muscle myogenesis by regulating myoblast differentiation.** *A*, Western blot analysis shows the shRNA-mediated down-regulation of MG53 in CHO cells. Lysates were prepared from CHO cells transfected with an MG53 expression vector and either shRNA-MG53 or nonspecific shRNA probe. Immunoblotting was performed with polyclonal anti-mouse body for MG53 (upper panel) or monoclonal antibody for  $\alpha$ -actin (lower panel). *B*, representative fluorescent microscope images of C2C12 cells at different days of differentiation (day 0, upper panel; day 5, middle panel; day 10, lower panel) to illustrate the absence of myotube formation in cells transfected with shRNA-MG53 (right panel) compared with the nonspecific shRNA (left panel). Scale bar, 50  $\mu$ m. *C*, statistical analysis of the down-regulation of MG53 inhibiting myotube formation at 5 or 10 days (\*,  $p < 0.01$ ; \*\*,  $p < 0.001$  by *t* test) compared with the control. The ratio of green myotubes to all green cells was defined as the percentage of myotubes. Data are represented as mean with S.E. cont, control.



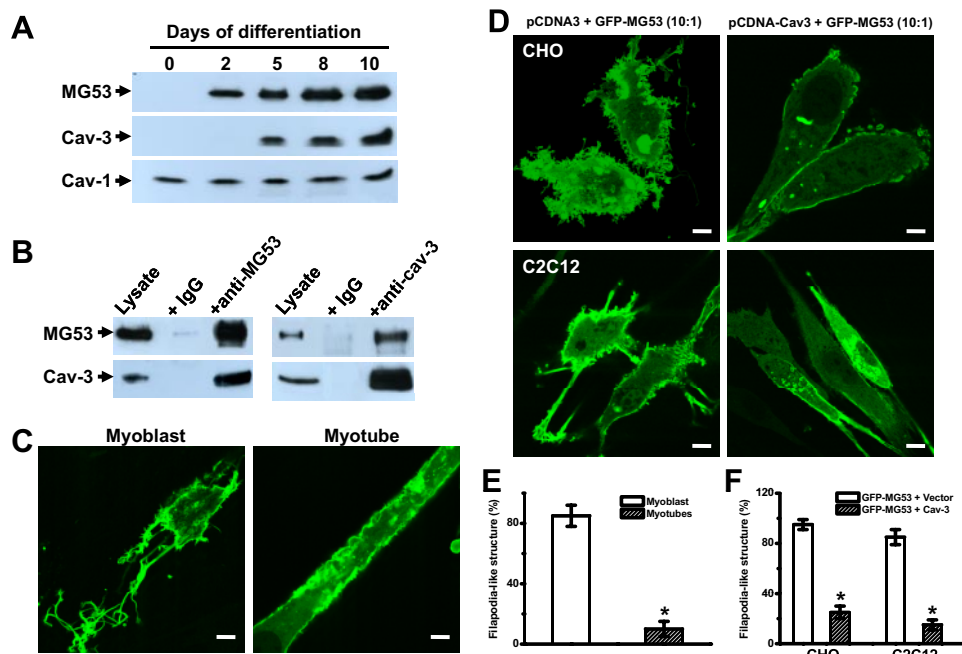


**FIGURE 4. Functional interaction between MG53 and caveolin-3 regulates dynamic membrane budding process in skeletal muscle.** A, Western blot analysis of the expression level of MG53 (upper panel), caveolin-3 (middle panel), and caveolin-1 (lower panel) during C2C12 cell differentiation at the indicated time following induction of differentiation (days 0, 2, 5, 8, and 10). B, whole cell lysate from mouse gastrocnemius skeletal muscle was subjected to co-immunoprecipitation with anti-MG53 (rabbit polyclonal antibody), anti-caveolin-3 (mouse monoclonal antibody), normal rabbit IgG as a negative control, and cell lysate as loading control. C, confocal images to illustrate the disappearance of filopodia-like structures during the process of C2C12 myotube formation (right panel) compared with myoblasts (left panel). Notice that intracellular vesicles positive for GFP-MG53 are still present in transfected C2C12 myotubes. D, overexpression of caveolin-3 in C2C12 myoblast cells (upper panel) or C2C12 myoblast cells (lower panel) were co-transfected with pcDNA-Cav3 and GFP-MG53 (10:1) (right panel) or co-transfected with pcDNA mock vector or GFP-MG53 (10:1) as control (left panel). Confocal images were taken at 48 h after transfection. Scale bar, 10  $\mu$ m. E and F, statistical analysis for C and D. The ratio of cells displaying filopodia-like structures to all green cells was defined as the filopodia-like structure percentage. Data are represented as mean with S.E. (\*,  $p < 0.01$  by t test).

**Muscle**—Our findings suggest that overexpression of MG53 can drive active membrane fusion and budding in both muscle and non-muscle cells and that down-regulation of MG53 results in compromised capacity of myotube differentiation. Further understanding of the physiological function of MG53 requires examination of how MG53-mediated membrane recycling contributes to the normal muscle differentiation process and what accessory factors regulate MG53 function in myogenesis.

As shown in Fig. 4A, MG53 expression was associated with C2C12 myotube differentiation. The expression of MG53 is absent in myoblast stage and is induced following initiation of differentiation. Interestingly expression of caveolin-3, a muscle-specific caveolin isoform associated with muscle differentiation (25, 26), follows the initiation of MG53 expression. The specific role of caveolin-3 in muscle differentiation is evidenced by the continuous presence of caveolin-1, a ubiquitous structural protein associated with caveolae in all cell types, throughout all stages of C2C12 differentiation. Using a co-immunoprecipitation assay, we found that MG53 can physically interact with caveolin-3 (Fig. 4B).

It is interesting to note that the distinct filopodia-like structures appearing in C2C12 myoblast overexpressing MG53 disappeared following differentiation of these myoblasts into myotubes (Fig. 4, C and E). Because filopodia-like structures are not

observed in either myoblasts that contain no endogenous MG53 or mature muscle fibers that contain endogenous MG53, the action of MG53 may be controlled by repression of MG53 expression in myoblasts and/or by regulatory mechanisms in mature myotubes and adult muscle fibers that may involve accessory proteins. Because caveolin-3 is developmentally regulated and can interact with MG53, we tested whether MG53-induced filopodia-like structure in C2C12 myoblasts or CHO cells could be influenced by the overexpression of caveolin-3.

As shown in Fig. 4D, concurrent overexpression of caveolin-3 and MG53 in either C2C12 myoblasts or CHO cells led to remarkable inhibition of the appearance of filopodia-like structures associated with GFP-MG53 overexpression. On average, CHO cells or C2C12 myoblasts transfected with caveolin-3 and GFP-MG53 (in a ratio of 10:1) exhibited  $74 \pm 5$  and  $82 \pm 6\%$  reduction in the appearance of filopodia-like structures, respectively. These results suggest that caveolin-3 represents one of the molecular regulators of MG53-me-

diated membrane fusion events.

**Down-regulation of Caveolin-3 Inhibits Myoblast Differentiation into Myotubes without Affecting Filopodia-like Structures Induced by GFP-MG53 Overexpression**—To further investigate the role of caveolin-3 in the subcellular distribution of MG53 and the formation of filopodia-like structures, we constructed a caveolin-3 shRNA plasmid that includes an independent red fluorescence protein expression cassette to provide a marker for shRNA transfected cells. Western blot analysis shown in Fig. 5A revealed that the shRNA-cav3 probe can suppress caveolin-3 expression in CHO cells transiently transfected with the caveolin-3 cDNA without affecting the expression of caveolin-1.

Although C2C12 myoblasts transfected with a nonspecific shRNA exhibited a normal differentiation pattern as shown by the abundant red fluorescence-labeled myotubes in Fig. 5B (left panel), acute suppression of caveolin-3 could significantly inhibit the differentiation of C2C12 myoblasts into myotubes (Fig. 5B, right panel). On average, less than 10% of the shRNA-cav3-transfected myoblasts marked by red fluorescence could differentiate into mature myotubes at day 6 after application of differentiation media (Fig. 5C). This result is consistent with previous studies by other investigators, who showed that the expression of caveolin-3 is essential for differentiation of C2C12 myotubes (25, 26).

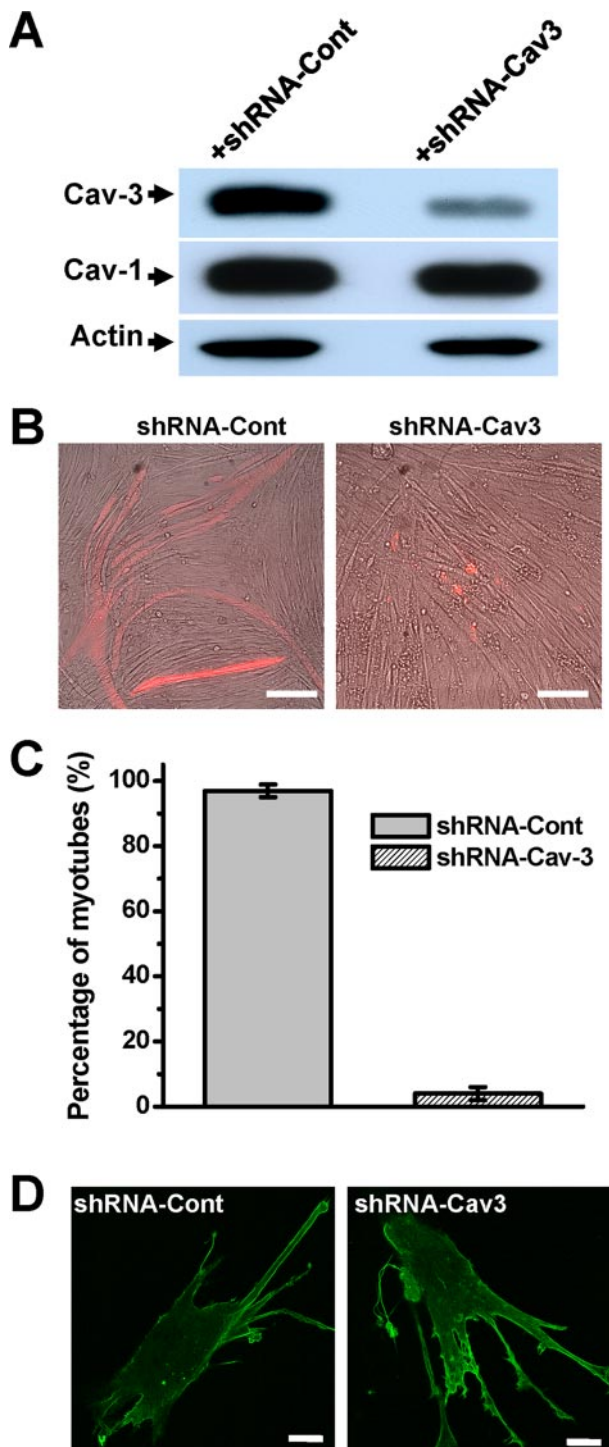


**FIGURE 5. shRNA-mediated suppression of caveolin-3 expression affects the myotube formation.** *A*, knockdown of caveolin-3 expression was analyzed by Western blot after transfection with shRNA-cav3 in C2C12 myotubes (6 days after differentiation). Cells transfected with the nonspecific shRNA plasmid acted as a control (Cont). *B*, down-regulation of caveolin-3 (right panel) by shRNA inhibits myotube formation compared with the control shRNA (left panel). Red fluorescence indicates the transfected cells. Fluorescence microscopy images were taken at 6 days after differentiation induction. Scale bar, 20  $\mu$ m. *C*, statistical analysis shows that down-regulation of caveolin-3 significantly inhibits myotube formation at 6 days (\*,  $p < 0.001$  by  $t$  test) compared with the control. The ratio of red fluorescent myotubes to all red fluorescent cells served as the percentage of myotubes. Data are represented as mean with S.E. *D*, confocal images of C2C12 myoblasts with co-expression of both GFP-MG53 and shRNA-cav3 (right panel) reveal no significant changes on the filopodia-like structures induced by GFP-MG53 or on the distribution of GFP-MG53 compared with the control shRNA (left panel). Scale bar, 5  $\mu$ m.

Confocal microscopic imaging showed that transfection of shRNA-cav3 into C2C12 myoblasts did not appear to affect the subcellular distribution of GFP-MG53 expressed in these cells (Fig. 5*D*). In particular, the distinct pattern of vesicular distribution of GFP-MG53 and filopodia-like membrane structures remained unaffected by the transient transfection with either shRNA-cav3 or the nonspecific shRNA. This result is consistent with the lack of expression of caveolin-3 in the myoblast stage of C2C12 cells.

The efficacy of the shRNA-cav3 probe to knock down the expression of caveolin-3 in C2C12 myotubes is difficult to assess because of the intrinsic role of caveolin-3 in mediating myotube formation (Fig. 5*B*). This also complicates analysis of the functional interaction between MG53 and caveolin-3; however, additional chemical means can be used to affect caveolin-3 organization in cell membranes.

**MG53-mediated Exocytosis Is Enhanced by Extraction of Cell Membrane Cholesterol with Methyl- $\beta$ -cyclodextrin**—Because of the essential nature of caveolin-3 in myotube differentiation, we tested the effect of methyl- $\beta$ -cyclodextrin (M- $\beta$ -CD) on C2C12 myoblasts overexpressing GFP-MG53 to further assay the functional impact of MG53-caveolin interaction on membrane recycling. M- $\beta$ -CD can extract cholesterol from cell membranes and has been widely used as an agent to disrupt caveolae structures (27). As shown in Fig. 6*A*, myoblasts overexpressing GFP-MG53 exhibited spontaneous fusion of vesicles both intracellularly as well as at the sarcolemmal membrane (see supplemental movie 1). These spontaneous fusion events were slow and occurred in the order of minutes. Following treatment with M- $\beta$ -CD, exocytotic events became greatly enhanced resulting in accelerated membrane fusion and massive budding of membrane vesicles (Fig. 6*B*). These initial alterations were rapidly induced, and extended incubation with M- $\beta$ -CD resulted in solubilization of GFP-MG53 within the myoblast (Fig. 6*C*). For visualization of the dynamic changes of membrane fusion events induced by M- $\beta$ -CD treatment, please see supplemental movie 2. These results re-enforce our observation that caveolin-mediated internalization of membrane vesicles likely play a regulatory role in preventing excessive exocytosis generated by MG53 overexpression.

**TRIM and SPRY Domains of MG53 Contribute Differentially to Membrane Targeting and Trafficking**—Our observation shown in Fig. 1*C* revealed a remarkable polarity of GFP fusion to MG53 in the intracellular distribution of MG53. In particular, fusion of GFP to the carboxyl-terminal end of MG53 altered the ability of MG53 to partition to the vesicular compartment and to target to sarcolemmal membrane. To further test the function of the TRIM and SPRY domains in facilitating the membrane fusion function of MG53, we generated a series of deletion mutants coupled to GFP (Fig. 7*A*).

To analyze the subcellular localization of these mutant constructs of MG53, confocal microscopic imaging was applied to C2C12 myoblasts following transient expression. As shown in Fig. 7*B* (right panels), GFP-TRIM or TRIM-GFP were predominantly localized to intracellular vesicles without apparent labeling of sarcolemmal membrane. This result suggests that the SPRY domain, which is absent from GFP-TRIM or TRIM-GFP, is necessary for targeting of MG53 to sarcolemmal mem-



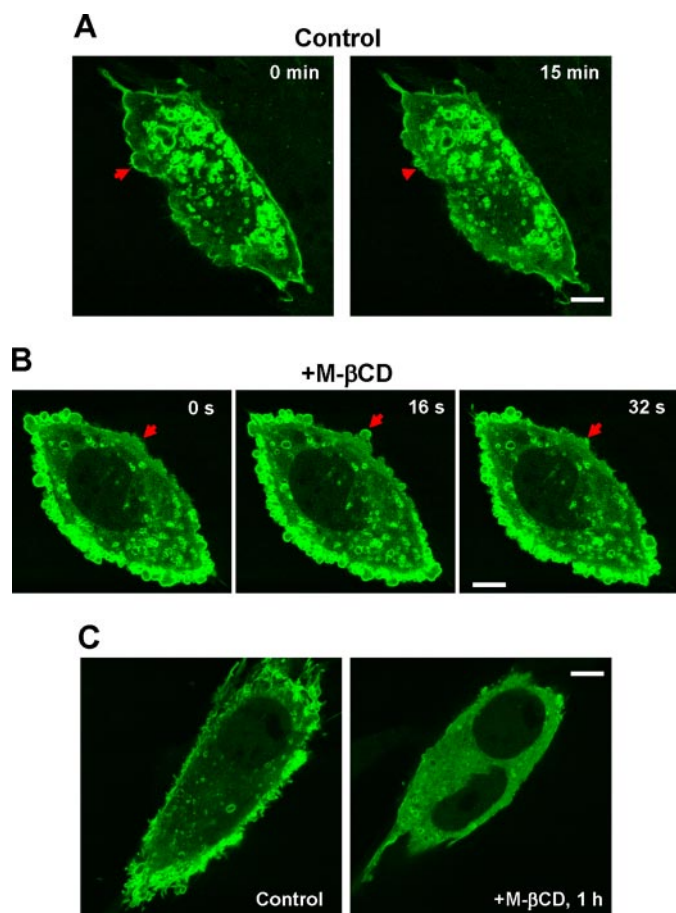


**FIGURE 6. Treatment of cells with methyl-β-cyclodextrin leads to increased exocytosis and solubilization of GFP-MG53 in C2C12 myoblasts.** *A*, representative confocal images to illustrate the spontaneous vesicle fusion and budding off from the membrane at the indicated time points (0 min, left panel; 15 min, right panel). *B*, confocal images to illustrate the GFP-MG53-labeled intracellular vesicles budding off from the membrane quickly after treatment with 10 mM M-βCD at the indicated time points (0 s, left panel; 16 s, middle panel; 32 s, right panel). See supplemental movies 1 and 2 for the dynamic changes in membrane trafficking events. *C*, confocal images to show the solubilization of GFP-MG53 after prolonged treatment with 10 mM M-βCD at room temperature for 1 h (right panel) compared with the same cell before treatment (left panel). Scale bar, 5 μm.

brane. The fact that MG53-GFP exhibited a predominantly cytosolic distribution (Fig. 7*B*, left panel) further supports the role of SPRY in targeting MG53 to the cell surface membrane.

Interestingly although GFP-SPRY or SPRY-GFP displayed a predominantly cytosolic pattern of distribution, they are clearly excluded from intracellular vesicles (Fig. 7*B*, middle panels). The cytosolic distribution pattern coupled with the exclusion of localization at intracellular vesicles of GFP-SPRY and SPRY-GFP likely reflects the role of TRIM. Presumably the TRIM motif can mediate the adherence of MG53 to intracellular vesicles (Fig. 7*B*, right panels). The SPRY domain is insufficient to target to the sarcolemma by itself; therefore the TRIM domain must be present in tandem with the SPRY domain for proper trafficking of MG53 to sarcolemmal membrane. In addition, our co-immunoprecipitation data show that caveolin-3 interacts with the TRIM motif of MG53 (Fig. 7*C*). Thus, it is possible that the functional interaction between MG53 and caveolin-3 may underlie some of the cellular factors contributing to the

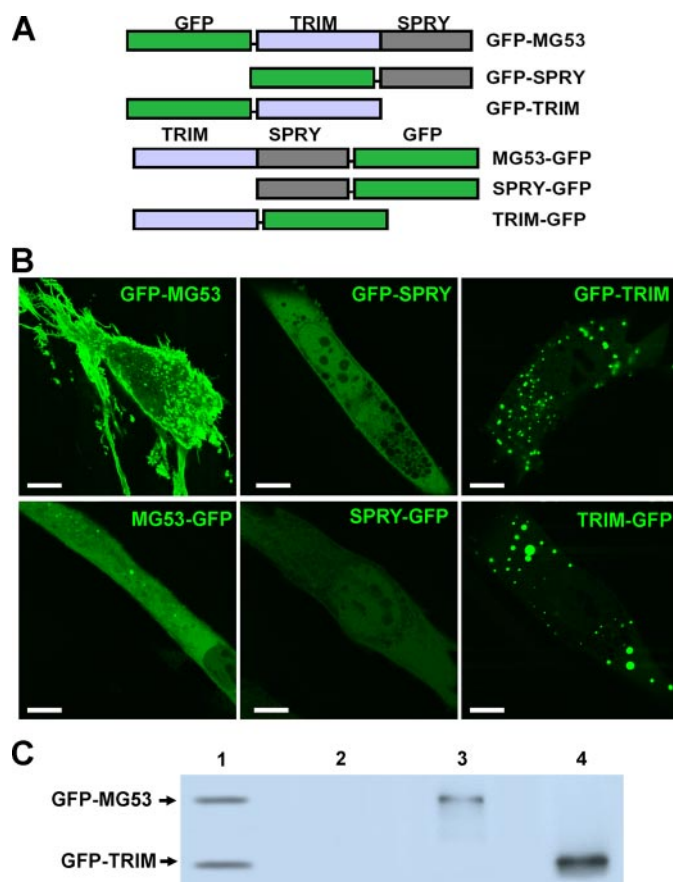


**FIGURE 7. Role of TRIM and SPRY domains in targeting of MG53 to the cell surface membrane.** *A*, scheme of the MG53 deletion constructs with GFP fused to the amino terminus or carboxyl terminus. "TRIM" represents amino acids 1–287, and "SPRY" represents amino acids 288–477. *B*, representative confocal images showing intracellular localization of each deletion construct. Scale bar, 5 μm. *C*, MG53 interacts with caveolin-3 through the TRIM motif. Cell lysate from CHO cells co-transfected with GFP-MG53 or GFP-TRIM and caveolin-3 was subjected to immunoprecipitation with anti-caveolin-3 (mouse monoclonal antibody). Lane 1, mixed cell lysate as positive control; lane 2, normal mouse IgG as negative control; lane 3, lysate from cells overexpressing GFP-MG53; lane 4, lysate from cells overexpressing GFP-TRIM.

diffuse pattern of GFP-SPRY and SPRY-GFP in C2C12 myoblasts.

Overall the regulated distribution of MG53 to the cell surface and intracellular compartments would likely result from coordinated action between the TRIM and SPRY domains. This requirement for both TRIM and SPRY for proper MG53 subcellular localization also has apparent functional significance as none of these deletion mutants display the filopodia-like structures or the robust vesicle budding events observed from overexpression of full-length MG53.

## DISCUSSION

Fusion, budding, and internalization of cell surface membranes are active cellular processes involved in a wide variety of physiological functions. Disruption of these membrane-re modeling mechanisms can result in a loss of membrane integrity and defective cell signaling pathways. Although muscle cells are traditionally thought to be terminally differentiated, extensive remodeling of sarcolemmal membrane still takes place under physiological and pathophysiological conditions, including trafficking and internalization of membrane trans-

porters and muscle fiber regeneration following injury or denervation (28, 29). The molecular machinery that regulates this process during development, disease, and senescence is not well understood. Here we show that a novel TRIM/RBCC family member protein, MG53, is a key component in driving membrane fusion, budding, and exocytosis. MG53 is unique in that it is only observed in striated muscle cells, and in contrast to most other defined TRIM/RBCC members, it is intimately associated with membrane trafficking.

The TRIM family of proteins is large and displays diverse cell biological functions (12, 30). Previous studies have linked TRIM protein function to several human diseases, including muscular dystrophy, viral infection, and cancer progression (9). Attempts at understanding the cell biological function of TRIM proteins have focused on the role of various protein motifs in mediating intracellular signaling events. For example, the coiled coil motif has been shown to facilitate protein dimerization, a characteristic required for coordinated function of TRIM proteins (31, 32). The RING and B-box motifs contain intrinsic E3 ligase enzymatic activity, which has been shown to regulate protein degradation in many cell types (33), particularly in the progression of muscle atrophy (12). Previous studies have also linked TRIM proteins to neuronal outgrowth and structural plasticity (34) as well as synaptic vesicle exocytosis (35). Because a limited number of the TRIM family members contain a carboxyl-terminal SPRY domain, the function of the SPRY domain has only recently been examined (14, 36–38). Several studies have suggested that a variable region within the SPRY domain of TRIM5 $\alpha$  in rhesus monkeys can mediate immunity to human immunodeficiency virus infection (13–15, 37). The MG53 gene identified in our study belongs to this TRIM subfamily containing a SPRY domain. Our studies with MG53 reveal a new cell biological function for the TRIM protein family in striated muscle that involves membrane remodeling and signaling that is dependent on the presence of a SPRY domain in tandem with the TRIM motif.

Our previous studies showed that MG53 can function in the repair of sarcolemmal membrane following acute cell injury (22). Those findings are consistent with our observation here that MG53 participates in vesicle trafficking in the course of normal cellular physiology. It has been suggested previously that the cell membrane repair process is an emergency response by the cell where cellular components with a certain role in the course of normal cell function are repurposed to act in the resealing of damaged cell membranes (39). Considering that translocation of intracellular vesicles to injury sites on the cell membrane would be an essential step in repair of the membrane, a role for MG53 in the normal process of intracellular vesicle trafficking seems to be in agreement with another critical function in repairing potentially catastrophic injury to muscle cells.

Based on our electron and confocal microscopic results, we found that MG53 is tethered to intracellular vesicles that traffic between different subcellular compartments with the majority of the protein restricted to a space near sarcolemmal membrane. MG53 can drive the active exocytotic process in both excitable and non-excitable cells as evidenced by the appearance of filopodia-like structures in cells overexpressing either

MG53 or GFP-MG53. In skeletal muscle, MG53 appears to contribute to myogenesis as RNA interference-mediated suppression of MG53 attenuated myoblast fusion and myotube formation. These findings should provide new insights into our understanding of TRIM protein function.

The primary amino acid sequence of MG53 contains no transmembrane domains or lipid modification motifs, suggesting that the localization of MG53 may involve interaction with accessory proteins. Through biochemical studies we found that MG53 can interact with caveolin-3, a muscle-specific protein associated with caveolae. Expression of MG53 precedes the appearance of caveolin-3 during myogenic differentiation of C2C12 cells. Thus, caveolin-3 may represent a regulatory factor that moderates the robust membrane trafficking events generated by the presence of MG53. We show that overexpression of caveolin-3 can down-regulate membrane budding induced by MG53 overexpression and prevent the formation of filopodia-like structures.

For maintenance of muscle membrane integrity, a balance of exocytosis and membrane internalization must be well controlled under physiologic conditions. The identified MG53-caveolin interaction has important implications for muscle physiology and pathophysiology. Extensive studies have linked caveolin-3 to muscle differentiation (40). Limb-girdle muscular dystrophy is associated with a mutation in caveolin-3 that leads to loss of ~95% of caveolin-3 expression. A caveolin-3-null mutation in mice produces defects in skeletal muscle membrane trafficking and a concurrent disruption of transverse tubule membrane organization (40–42), phenotypes that are associated with limb-girdle muscular dystrophy. Interestingly transgenic overexpression of caveolin-3 has also been shown to result in severe muscular degeneration similar to Duchenne muscular dystrophy (43). Therefore, caveolin-3 function appears to be essential for myogenesis and maintenance of muscle integrity. Our results suggest that caveolin-3 expression can control MG53 activity. Presumably some aspects of caveolin-3 function may involve its interaction with MG53, so the loss of caveolin-3 in development may lead to aberrant MG53-mediated membrane remodeling. One can envision that targeting MG53-caveolin3 interaction would represent an effective therapy for muscle-related disease involving altered membrane structures.

Trafficking of intracellular vesicles containing MG53 to sarcolemmal membrane requires coordinated function of the TRIM and SPRY domains. Our studies show that the SPRY domain is essential for targeting of MG53 to the cell membrane, whereas the TRIM domain mediates interaction with intracellular vesicles in the context of the MG53 molecule. These results not only demonstrate the importance of a coordinated action of TRIM and SPRY to facilitate membrane trafficking properties of MG53, but they also suggest the possibility that other TRIM family proteins carrying a similar SPRY domain may also exhibit membrane-modifying properties. Indeed a previous study by Perez-Caballero *et al.* (44) demonstrated that both TRIM and SPRY domains of TRIM5 $\alpha$  are required to provide cellular resistance to retroviral infection, although the membrane trafficking properties of TRIM5 $\alpha$  have yet to be examined. It remains to be determined whether TRIM-SPRY



intermolecular interactions produce intrinsic membrane targeting ability or whether additional cellular factors beyond caveolin-3 are required.

In conclusion, we have shown that MG53 is an active component of membrane fusion, exocytosis, and vesicle budding that play an important role in myogenesis of striated muscle cells. The presence of the TRIM and SPRY motif in MG53 and a functional interaction with caveolin-3 are essential in regulating membrane trafficking and cellular signaling events across sarcolemmal membrane.

## REFERENCES

- Flucher, B. E., Phillips, J. L., Powell, J. A., Andrews, S. B., and Daniels, M. P. (1992) *Dev. Biol.* **150**, 266–280
- Franzini-Armstrong, C., and Protasi, F. (1997) *Physiol. Rev.* **77**, 699–729
- Moyers, J. S., Bilan, P. J., Reynet, C., and Kahn, C. R. (1996) *J. Biol. Chem.* **271**, 23111–23116
- Song, K. S., Scherer, P. E., Tang, Z., Okamoto, T., Li, S., Chafel, M., Chu, C., Kohtz, D. S., and Lisanti, M. P. (1996) *J. Biol. Chem.* **271**, 15160–15165
- Huang, J., Imamura, T., and Olefsky, J. M. (2001) *Proc. Natl. Acad. Sci. U. S. A.* **98**, 13084–13089
- Scriven, D. R., Klimek, A., Asghari, P., Bellve, K., and Moore, E. D. (2005) *Biophys. J.* **89**, 1893–1901
- Bolanos-Jimenez, F., Bordais, A., Behra, M., Strahle, U., Mornet, D., Sahel, J., and Rendon, A. (2001) *Gene (Amst.)* **274**, 217–226
- Ho, M., Post, C. M., Donahue, L. R., Lidov, H. G., Bronson, R. T., Goolsby, H., Watkins, S. C., Cox, G. A., and Brown, R. H., Jr. (2004) *Hum. Mol. Genet.* **13**, 1999–2010
- Meroni, G., and Diez-Roux, G. (2005) *BioEssays* **27**, 1147–1157
- Ponting, C., Schultz, J., and Bork, P. (1997) *Trends Biochem. Sci.* **22**, 193–194
- Vichi, A., Payne, D. M., Pacheco-Rodriguez, G., Moss, J., and Vaughan, M. (2005) *Proc. Natl. Acad. Sci. U. S. A.* **102**, 1945–1950
- Kudryashova, E., Kudryashov, D., Kramerova, I., and Spencer, M. J. (2005) *J. Mol. Biol.* **354**, 413–424
- Keckesova, Z., Ylinen, L. M., and Towers, G. J. (2004) *Proc. Natl. Acad. Sci. U. S. A.* **101**, 10780–10785
- Javanbakht, H., Diaz-Griffero, F., Stremlau, M., Si, Z., and Sodroski, J. (2005) *J. Biol. Chem.* **280**, 26933–26940
- Sawyer, S. L., Wu, L. I., Emerman, M., and Malik, H. S. (2005) *Proc. Natl. Acad. Sci. U. S. A.* **102**, 2832–2837
- Weisleder, N., Takeshima, H., and Ma, J. (2008) *Cell Calcium* **43**, 1–8
- Ito, K., Komazaki, S., Sasamoto, K., Yoshida, M., Nishi, M., Kitamura, K., and Takeshima, H. (2001) *J. Cell Biol.* **154**, 1059–1067
- Takeshima, H., Komazaki, S., Nishi, M., Iino, M., and Kangawa, K. (2000) *Mol. Cell* **6**, 11–22
- Hirata, Y., Brotto, M. D., Weisleder, N., Chu, Y., Lin, P., Zhao, X., Thornton, A., Komazaki, S., Takeshima, H., Ma, J., and Pan, Z. (2006) *Biophys. J.* **90**, 4418–4427
- Nishi, M., Komazaki, S., Kurebayashi, N., Ogawa, Y., Noda, T., Iino, M., and Takeshima, H. (1999) *J. Cell Biol.* **147**, 1473–1480
- Pan, Z., Yang, D., Nagaraj, R. Y., Nosek, T. A., Nishi, M., Takeshima, H., Cheng, H., and Ma, J. (2002) *Nat. Cell Biol.* **4**, 379–383
- Cai, C., Masumiya, H., Weisleder, N., Matsuda, N., Nishi, N., Hwang, M., Ko, J., Lin, P., Thornton, A., Zhao, X., Pan, Z., Komazaki, S., Brotto, M., Takeshima, H., and Ma, J. (2009) *Nat. Cell Biol.* **11**, 56–64
- Takeshima, H., Shimuta, M., Komazaki, S., Ohmi, K., Nishi, M., Iino, M., Miyata, A., and Kangawa, K. (1998) *Biochem. J.* **331**, 317–322
- Komazaki, S., Nishi, M., Kangawa, K., and Takeshima, H. (1999) *Dev. Dyn.* **215**, 87–95
- Parton, R. G., Way, M., Zorzi, N., and Stang, E. (1997) *J. Cell Biol.* **136**, 137–154
- Galbiati, F., Volonte, D., Engelman, J. A., Scherer, P. E., and Lisanti, M. P. (1999) *J. Biol. Chem.* **274**, 30315–30321
- Smith, R. D., Babychuk, E. B., Noble, K., Draeger, A., and Wray, S. (2005) *Am. J. Physiol.* **288**, C982–C988
- Valentine, B. A., Cooper, B. J., Cummings, J. F., and de Lahunta, A. (1990) *J. Neurol. Sci.* **97**, 1–23
- Fiori, M. G., Salvi, F., Plasmati, R., and Tassinari, C. A. (1996) *Clin. Neuropathol.* **15**, 240–247
- Wang, Y., Li, Y., Qi, X., Yuan, W., Ai, J., Zhu, C., Cao, L., Yang, H., Liu, F., Wu, X., and Liu, M. (2004) *Biochem. Biophys. Res. Commun.* **323**, 9–16
- Chakrabarty, T., Xiao, M., Cooke, R., and Selvin, P. R. (2002) *Proc. Natl. Acad. Sci. U. S. A.* **99**, 6011–6016
- Ward, N. L., Van Slyke, P., and Dumont, D. J. (2004) *Biochem. Biophys. Res. Commun.* **323**, 937–946
- Wei, X., Yu, Z. K., Ramalingam, A., Grossman, S. R., Yu, J. H., Bloch, D. B., and Maki, C. G. (2003) *J. Biol. Chem.* **278**, 29288–29297
- van Diepen, M. T., Spencer, G. E., van Minnen, J., Gouwenberg, Y., Bouwman, J., Smit, A. B., and van Kesteren, R. E. (2005) *Mol. Cell. Neurosci.* **29**, 74–81
- Li, Y., Chin, L. S., Weigel, C., and Li, L. (2001) *J. Biol. Chem.* **276**, 40824–40833
- Rhodes, D. A., de Bono, B., and Trowsdale, J. (2005) *Immunology* **116**, 411–417
- Nakayama, E. E., Miyoshi, H., Nagai, Y., and Shioda, T. (2005) *J. Virol.* **79**, 8870–8877
- Song, B., Gold, B., O'Huigin, C., Javanbakht, H., Li, X., Stremlau, M., Winkler, C., Dean, M., and Sodroski, J. (2005) *J. Virol.* **79**, 6111–6121
- McNeil, P. L., and Kirchhausen, T. (2005) *Nat. Rev. Mol. Cell Biol.* **6**, 499–505
- Volonte, D., Peoples, A. J., and Galbiati, F. (2003) *Mol. Biol. Cell* **14**, 4075–4088
- Galbiati, F., Engelman, J. A., Volonte, D., Zhang, X. L., Minetti, C., Li, M., Hou, H., Jr., Kneitz, B., Edelmann, W., and Lisanti, M. P. (2001) *J. Biol. Chem.* **276**, 21425–21433
- Oshikawa, J., Otsu, K., Toya, Y., Tsunematsu, T., Hankins, R., Kawabe, J., Minamisawa, S., Umemura, S., Hagiwara, Y., and Ishikawa, Y. (2004) *Proc. Natl. Acad. Sci. U. S. A.* **101**, 12670–12675
- Galbiati, F., Volonte, D., Chu, J. B., Li, M., Fine, S. W., Fu, M., Bermudez, J., Pedemonte, M., Weidenheim, K. M., Pestell, R. G., Minetti, C., and Lisanti, M. P. (2000) *Proc. Natl. Acad. Sci. U. S. A.* **97**, 9689–9694
- Perez-Caballero, D., Hatzioannou, T., Yang, A., Cowan, S., and Bieniasz, P. D. (2005) *J. Virol.* **79**, 8969–8978